Free volume of an epoxy resin and its relation to structural relaxation: Evidence from positron lifetime and pressure-volume-temperature experiments

Günter Dlubek*
ITA Institut für Innovative Technologien, Köthen/Halle, Wiesenring 4, D-06120 Lieskau (Halle/S.), Germany

E. M. Hassan and Reinhard Krause-Rehberg
Martin-Luther-Universität Halle-Wittenberg, Fachbereich Physik, D-06099 Halle/S., Germany

Jürgen Pionteck
Leibniz-Institut für Polymerforschung Dresden e.V., Hohe Strasse 6, D-01069 Dresden, Germany
(Received 10 October 2005; published 3 March 2006)

The microstructure of the free volume and its temperature dependence in the epoxy resin diglycidyl ether of bisphenol-A (DGEBA) have been examined using positron annihilation lifetime spectroscopy (PALS, 80–350 K, 10^{-5} Pa) and pressure-volume-temperature (PVT, 293–470 K, 0.1–200 MPa) experiments. Employing the Simha-Somcynsky lattice-hole theory (S-S eos), the excess (hole) free volume fraction h and the specific free and occupied volumes, $V_f=hV$ and $V_{\mathrm{occ}}=(1-h)V$, were estimated. From the PALS spectra analyzed with the new routine LT9.0 the hole size distribution, its mean, $\langle v_h\rangle$, and mean dispersion, σ_h, were calculated. $\langle v_h\rangle$ varies from 35 to 130 Å^3. From a comparison of $\langle v_h\rangle$ with V and V_f, the specific hole number N_h' was estimated to be independent of the temperature $[N_h(300\ \mathrm{K})=N_h'/V=0.65\ \mathrm{nm}^{-3}]$. From comparison with reported dielectric and viscosity measurements, we found that the structural relaxation slows down faster than the shrinkage of the hole free volume V_f would predict on the basis of the free volume theory. Our results indicate that the structural relaxation in DGEBA operates via the free-volume mechanism only when liquidlike clusters of cells of the S-S lattice appear which contain a local free volume of ~1.5 or more empty S-S cells. The same conclusion follows from the pressure dependency of the structural relaxation and V_f. It is shown that PALS mirrors thermal volume fluctuations on a subnanometer scale via the dispersion in the ortho-positronium lifetimes. Using a fluctuation approach, the temperature dependency of the characteristic length of dynamic heterogeneity, ξ, is estimated to vary from $\xi=1.9$ nm at T_g to 1.0 nm at $T/T_g>1.2$. A model was proposed which relates the spatial structure of the free volume as concluded from PALS to the known mobility pattern of the dynamic glass transition at low (cooperative α-relaxation) and high (a-relaxation) temperatures. We discuss possible reasons for the differences between the results of our method and the conclusion from dynamic heat capacity.

DOI: 10.1103/PhysRevE.73.031803 PACS number(s): 61.41.+e, 64.70.Pf, 65.40.De, 78.70.Bj

INTRODUCTION

The fundamental mechanisms underlying the glass transition of a liquid or polymeric melt continue to be studied and are strongly debated [1–9]. In this field, some common aspects in the dynamics of different systems suggest that, despite material-specific aspects, some unitary basic interpretation should also be found. One common feature of the dynamics of a glass-forming liquid is the relation between the mobility of a certain species in the liquid (guest molecules, host molecules, chain segments) and the microstructure and amount of free volume [10–14]. Although very important, this aspect still provokes controversy when different interpretations are discussed [15–20].

When applying the free volume theory of Cohen and Turnbull [13] to a structural relaxation process in a liquid, its frequency ω is expressed by

$$\omega = C\exp(-\gamma V_f^*/V_f), \tag{1}$$

where V_f is the mean specific (not fractional) free volume of the liquid, γV_f^* is the minimum specific free volume required for the occurrence of the process, and $\gamma=0.5-1$. The free volume V_f in Eq. (1) is not equal to the total free volume, $V_{\mathrm{ft}}=V-V_W$ (V_W denotes van der Waals volume), but is a particular free volume appearing due to dynamic disorder in the liquid in excess of an occupied volume V_{occ}, $V_f=V-V_{\mathrm{occ}}$. We will denote this free volume as the hole free volume.

Assuming that the specific hole free volume of the liquid shows a linear expansion with the temperature,

$$V_f = E_f(T-T_0'), \tag{2}$$

where $E_f=dV_f/dT$ is its specific thermal expansivity and $T_0'<T_g$ is the temperature where the (extrapolated) free volume disappears, one obtains by substituting Eq. (2) into Eq. (1) the well known Vogel-Fulcher-Tammann (VFT) equation [21–24]

*Author to whom correspondence should be addressed. Electronic address: gdlubek@aol.com

$$\omega = \omega_0 \exp[-B/(T - T_0)]. \quad (3)$$

The constants correspond to $\omega_0 = C$, $B = B' = \gamma V_f^*/E_f$, and $T_0 = T_0'$ (T_0 is the Vogel temperature).

A realistic value of the specific hole free volume V_f can be determined from pressure-volume-temperature (PVT) experiments analyzed by employing the equation of state of the Simha-Somcynsky lattice-hole theory (S-S eos) [25–29]. Further information about the free volume may be obtained from positron annihilation lifetime spectroscopy (PALS) [30–34]. In amorphous polymers positronium (Ps), an electron-positron bound state is typically formed in a hole and stays there until annihilation (*Anderson* localization). Positrons contained within the *ortho*-state of positronium (*o*-Ps) preferentially annihilate with electrons other than their bound partners and with opposite spin during collisions with molecules in the hole wall. This reduces the *o*-Ps's lifetime from its value in a vacuum, 142 ns (self-annihilation), to the low-ns range (pick-off annihilation). The smaller the hole is, the higher the frequency of collisions and the shorter the *o*-Ps life. If the holes are spherical [30–32], cylindrical, or cuboidal [35,36] in shape, then the hole size can be calculated from the *o*-Ps lifetime using a semiempirical model.

PALS itself is able to measure the mean volume of the holes $\langle v_h \rangle$ and, with larger limitations, their size distribution (mean dispersion σ_h [37–41]). It is, however, unable to directly measure the hole density or the hole fraction. It was shown that a correlation of PALS results with the specific hole free volume V_f allows one to estimate the specific (*o*-Ps) hole density $N_h' = V_f/\langle v_h \rangle$ [39–44].

In the current work, we have studied the free volume of an epoxy resin and analyzed the reported dynamics [45–47] of this resin in terms of the free volume theory. The aim of our study is to characterize the free volume as complete as possible and to use this to test the validity of the Cohen-Turnbull free volume theory, to discover possible deviations from the expected behavior, and to discuss physical reasons for these deviations. To this aim, we have performed PVT [48] and PALS experiments.

To analyze the positron lifetime spectra, we used the new routine LIFETIME [49] in its latest version LT9.0 [50], which allows both discrete and log-normally distributed annihilation rates. From the distribution of the *o*-Ps annihilation rate, the size distribution of free volume holes can be calculated. The experiments have been used to estimate parameters characterizing the free volume such as V_f, $h = V_f/V$, $\langle v_h \rangle$, σ_h, and N_h'. Furthermore, we developed a fluctuation approach that allows us to estimate the temperature-dependent characteristic length of dynamic heterogeneity and the corresponding subvolume, respectively, from PALS data. Reasons for the differences between the conclusions from our method and the conclusion from dynamic heat capacity [1] are discussed.

The sample under investigation was the epoxy resin diglycidyl ether of bisphenol-A (DGEBA) in pure, uncured state. A very detailed study of the dynamics of this sample employing broadband dielectric spectroscopy, heat capacity spectroscopy (3ω method), and viscosimetry was published by Corezzi *et al.* [45]. These results and their careful analysis in terms of the VTF equation make the sample very attractive for the aim of our work. Recently, Beiner and Ngai [46] have discussed the interrelation between primary and secondary relaxations in neat and cured DGEBA. Moreover, Corezzi *et al.* [47] studied the pressure dependence of dielectric relaxation of this epoxy resin. We will involve also these data in our discussion.

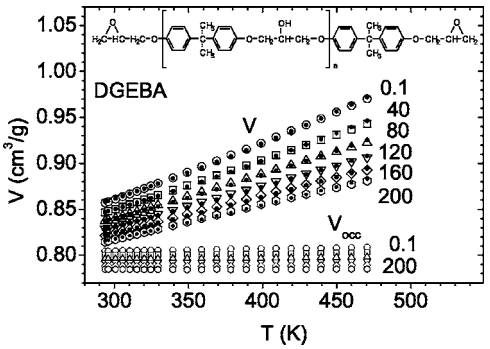

FIG. 1. Specific total, V, and occupied, $V_{occ} = (1-h)V$, volume of DGEBA as a function of temperature T and as selection of isobars (in MPa). The dots within the open symbols represent the fits of Eq. (5) to the volume data.

EXPERIMENT

The sample of DGEBA used in this study was the same as investigated by Corezzi *et al.* [45] and supplied by Beiner (Halle, Germany). It was purchased from Shell Co. under the trade name Epon 828 and had an average molecular weight of $\sim$380 g/mol, corresponding to $n \approx 0.14$ in the chemical formula reported in Fig. 1. The calorimetric glass transition temperature of this sample is 255 ± 1 K, obtained at a heating rate of 10 K/min.

Standard PVT experiments were carried out by means of a fully automated GNOMIX high-pressure dilatometer [48]. The data were collected in the range from 293 to 470 K in steps of 10($\pm$1) K. At each constant temperature the material was pressurized from 10 to 200 MPa and data were collected in steps of 10($\pm$0.1) MPa. The specific volumes for ambient pressure were obtained by extrapolating the values for 10 to 30 MPa in steps of 1 MPa according to the Tait equation using the standard GNOMIX PVT software. The instrument is able to detect changes in specific volume as small as 0.0002 $cm^3\ g^{-1}$ with an absolute accuracy of 0.002 $cm^3\ g^{-1}$. The pycnometric densities of the liquid resin was deterimned to be 1.1655 g cm^{-3} at 21.8 °C.

The PALS measurements were done using a fast-fast coincidence system [34] with a time resolution of 272 ps [full width at half-maximum (FWHM), ^{22}Na source] and an analyzer channel width of 12.8 ps. Two identical samples were sandwiched around a 1 MBq positron source: ^{22}NaCl, deposited between two 2-μm-thick aluminum foils. To prevent sticking of the source to the samples, each sample was held in a container of 2 mm width and 8×8 mm^2 area with a window made of foils of 8-μm-thick kapton and 7-μm-thick aluminum.

The temperature of the sample, placed in a vacuum chamber with a pressure of 10^{-5} Pa, was varied between 80 and

350 K in steps of 5 or 10 K, with an uncertainty of ±1 K. Before lowering the temperature, the samples were degassed and dried in vacuum for 18 h. Each measurement lasted 7 h leading to a lifetime spectrum of $\sim 5\times 10^6$ coincidence. Source corrections, 7.5% of 386 ps (kapton and NaCl) and 10.8% of 165 ps (Al foils), and time resolution were determined by measuring a defect-free p-type silicon reference (τ=219 ps). The final resolution function used in the spectrum analysis was determined as a sum of two Gaussians.

RESULTS AND DISCUSSION

Specific total, occupied, and free volume

Figure 1 shows a series of volume, V, isobars with the pressure, P, as the parameter. We have analyzed these data employing the S-S eos [25,28]. This theory describes the structure of a liquid by a cell or lattice model (coordination number of $z=12$) and models the disorder by assuming a statistical mixture of occupied (fraction y) and unoccupied cells (holes or vacancies, fraction $h=1-y$). The eos is represented in scaled form, with scaling parameters P^*, V^*, and T^*, in two coupled equations. One of these follows from the pressure equation $P=-(\partial F/\partial V)_T$, where $F=F(V,T,y)$ is the configurational (Helmholtz) free energy F of the liquid,

$$\frac{\tilde{P}\tilde{V}}{\tilde{T}} = [1 - y(2^{1/2}y\tilde{V})^{-1/3}]^{-1} + \frac{y}{\tilde{T}}[2.002(y\tilde{V})^{-4} - 2.409(y\tilde{V})^{-2}]. \tag{4}$$

Here $\tilde{P}$, $\tilde{V}$, and $\tilde{T}$ are the reduced variables, $\tilde{P}=P/P^*$, $\tilde{V}=V/V^*$, $\tilde{T}=T/T^*$. The occupied volume fraction y is coupled with $\tilde{T}$ and $\tilde{V}$ in a second equation derived from the minimization condition $(\partial F/\partial y)_{V,T}=0$. It was shown that both equations may be replaced in the temperature and pressure ranges $\tilde{T}=0.016-0.071$ and $\tilde{P}=0-0.35$ by the universal interpolation expression

$$\ln \tilde{V}(P,T) = a_0 + a_1\tilde{T}^{3/2} + \tilde{P}[a_2 + (a_3 + a_4\tilde{P} + a_5\tilde{P}^2)\tilde{T}^2]. \tag{5}$$

The molecular mass of the S-S lattice s-mer, M_0, is related to the scaling parameters via $M_0=(c/s)RT^*/P^*V^*$, where R is the gas constant. Here $3c$ is the number of external degrees of freedom per molecule. The flexibility parameter $3c/s$ defines the size of the s-mer and also the constants in Eq. (5). For rigid spherical molecules $s=1$ and $3c=3$, while for flexible chain molecules usually a value of $3c=s+3$ is *a priori* assumed. For polymers, $s\to\infty$ and $3c/s=1$ follows. The constants in Eq. (5), following the most recent determination by Utracki and Simha [28], are $a_0=-0.10346$, $a_1=23.854$, $a_2=-0.1320$, $a_3=-333.7$, $a_4=1032.5$, and $a_5=-1329.9$. We estimated the scaling parameters P^*, V^*, and T^* from consecutive nonlinear least-squares fits of Eq. (5) to the volume data assuming $3c/s=1$. From fits of the zero pressure isobars, $T^*=9941(\pm 20)$ K and $V^*=0.8432(\pm 0.003)$ cm^3/g were determined.

When assuming a flexibility parameter of $3c/s=3$, the parameters in Eq. (5) for $P=0$ are calculated to be $a_0=-0.0928$ and $a_1=17.508$ [51]. A tentative fit of Eq. (5) to our volume data gives then the scaling parameters $T^*=8088$ K and $V^*=0.8342$ cm^3/g, but the hole fraction $h=1-y$ calculated from Eq. (4) with this set of parameters is almost the same as before. This shows that the choice of the flexibility ratio $3c/s$ has no significant effect on our free volume results.

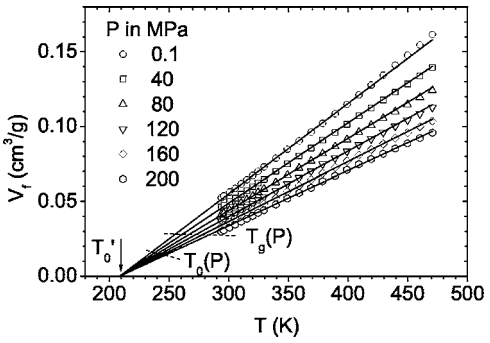

FIG. 2. The specific hole free volume $V_f=hV$ of DGEBA as a function of temperature T and as selection of isobars. The solid lines are due to fits of Eq. (6) to the data. T_0' is the temperature where the extrapolated hole free volume disappears. The dashed lines show the pressure dependency of the glass transition temperature $T_g(P)$ and Vogel temperature $T_0(P)$ of structural a'-relaxation (see text) estimated from dielectric relaxation experiments [15,45,47].

In a second fit including the data from the PVT field in the range from 10 to 200 MPa and fixing T^* and V^* to the former values, the scaling pressure $P^*=1190(\pm 20)$ MPa was estimated. Figure 1 shows the experimental volume data as well as the S-S eos fits as empty symbols and dots, respectively, and the corresponding specific occupied volume $V_{\rm occ}=yV$ as small empty symbols.

The coefficient of thermal expansion of the total volume, $\alpha=(1/V)(dV/dT)|_P$, increases at ambient pressure from 6.79 (T=293 K) to 7.19 (470 K) but decreases at P=200 MPa to values from 4.97 to 3.95, all in units of 10^{-4} K^{-1}. Unlike the total volume, the occupied volume shows almost no thermal expansion, $\alpha_{\rm occ}=(1/V_{\rm occ})(dV_{\rm occ}/dT)|_P=0.28\times 10^{-4}$ K^{-1} (P=0.1 MPa) and 0.17×10^{-4} K^{-1} (200 MPa) at 293 K. It is, however, remarkably compressible with a compressibility of $\kappa_{\rm occ}=-(1/V_{\rm occ})(dV_{\rm occ}/dP)|_T=1.36\times 10^{-4}$ MPa^{-1} for T=293 K and $\kappa_{\rm occ}=1.83\times 10^{-4}$ MPa^{-1} for 470 K, both values for P=0.1 MPa. These values are close to the compressibilities estimated for polyethylene crystals [52]. The compressibility of the occupied volume implies that the free volume $V_f=V-V_{\rm occ}$ may increase with increasing pressure for the same total volume V. The compressibility of the total volume at ambient pressure is $\kappa=3.32\times 10^{-4}$ MPa^{-1} for T=293 K and 7.95×10^{-4} MPa^{-1} for 470 K.

Figure 2 shows a series of selected isobars of the specific hole free volume $V_f=hV$. The increase in V_f with the temperature comes from an increase in the hole fraction, at ambient pressure from h=0.0613 at T=293 K to 0.1665 at 470 K. The corresponding increase at P=200 MPa is from h=0.0366 to 0.1089. The volume of a cell of the S-S lattice, $v_{\rm SS}$, varies as $V_{\rm occ}$, $v_{\rm SS}(T,P)=M_0V_{\rm occ}(T,P)/N_A$, and, therefore, exhibits almost no thermal expansion but is compress-

ible. For $T=293$ K one obtains values of $v_{SS}=38.3$ Å^3 for $P=0.1$ MPa and $v_{SS}=37.4$ Å^3 for $P=200$ MPa using the estimated $M_0=28.7$ g/mol. The decrease of V_f with increasing pressure P is therefore due to the decrease of both h and v_{SS}.

To find an algebraic expression, we fitted first the free volume isobars in Fig. 2 with the linear Eq. (2), $V_f=E_f(T-T_0')$, allowing E_f and T_0' to be free-floating fitting parameters. In a second fit, we fixed T_0' to its average value of $T_0'=209(\pm 3)$ K. Subsequently, we analyzed the pressure dependency of the specific thermal expansivity and found that E_f follows the function $E_f=E_{f0}/(1+aP)$. From our fits, the relation

$$V_f(T,P)=[E_{f0}/(1+aP)](T-T_0') \tag{6}$$

follows with the parameters $T_0'=209$ K, $E_{f0}=6.038(\pm 0.04)\times 10^{-4}$ cm^3 g^{-1} K^{-1}, and $a=3.168(\pm 0.05)\times 10^{-3}$ MPa^{-1}.

The extrapolation of the experimental data for ambient pressure to the glass transition temperature $T_g=255$ K using Eq. (6) gives values of $V_{fg}=0.0279$ cm^3/g and $h_g=V_{fg}/V_g=0.0334$. For polymers it was found that the hole fraction increases from $h_g\approx 0.02$ for materials with $T_g=200$ K to $h_g\approx 0.08$ with $T_g=400$ K [42]. The specific expansivity of the free volume, $E_f=dV_f/dT|_P$, increases at ambient pressure from $E_f=5.60\times 10^{-4}$ cm^3 g^{-1} K^{-1} ($T=293$ K) to 6.76×10^{-4} cm^3 g^{-1} K^{-1} (470 K). Since V_f increases faster than E_f, the coefficient of thermal expansion of the free volume, $\alpha_f=E_f/V_f|_P$, decreases with increasing temperature from 10.65×10^{-3} K^{-1} to 4.18×10^{-3} K^{-1}. The corresponding values at 200 MPa lie between 17.61×10^{-3} K^{-1} (293 K) and 5.51×10^{-3} K^{-1} (470) K. We remark that the specific expansivities E_i and the fractional coefficients of thermal expansion, defined by $\alpha_i^*=E_i/V$, but not the coefficients of thermal expansion, $\alpha_i=E_i/V_i$, behave additively: $E=E_{occ}+E_f$, $\alpha=\alpha_{occ}^*+\alpha_f^*$, but $\alpha=(1-h)\alpha_{occ}+h\alpha_f$.

From an Arrhenius plot of the hole fraction h at ambient pressure, we estimated the enthalpy of hole formation, $H_h=-k_B\partial \ln h/\partial(1/T)|_P$, to be 6.47($\pm$0.2) kJ/mol, which corresponds to approximately half of the cohesive energy of a mer of the S-S lattice. (For details of the calculation, see our previous papers [40,41].) This shows that the Schottky mechanism is active, i.e., a hole (vacancy) is formed by the migration of a mer to the surface (or, equivalently, by the diffusion of a vacancy from the surface into the bulk).

POSITRON LIFETIME SPECTRA AND THEIR ANALYSIS

The positron lifetime spectrum $s(t)$ is given by the Laplace transformation of the function $\alpha(\lambda)\lambda$, where $\alpha(\lambda)$ is the probability density function (pdf) of the annihilation rate $\lambda=1/\tau$. It shows three decay channels which come from the annihilation of *para* positronium (*p*-Ps, τ_1), free (not Ps) positrons (e^+, τ_2), and *ortho* positronium (*o*-Ps, τ_3; $\tau_1<\tau_2<\tau_3$, their relative intensities are $I_1+I_2+I_3=1$) [33,34]. The new routine LT9.0 [49,50] which we used for the analysis of lifetime spectra assumes that the function $\alpha_i(\lambda)\lambda$ follows a log-normal distribution where $\alpha_i(\lambda)$ is the pdf of annihilation rates of the decay channel i. In order to make the numerical analysis more stable, we assumed that the lifetime spectrum

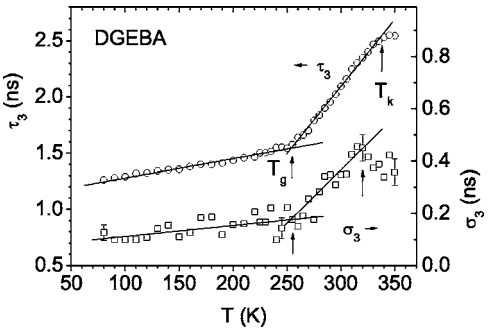

FIG. 3. Mean, τ_3, and mean dispersion, σ_3, of the *o*-Ps lifetime in DGEBA. The lines through data points are a visual aid, the arrows indicate the glass transition, T_g, and the "knee" temperature T_k. The statistical errors of τ_3 are smaller than the symbol size.

of *p*-Ps ($i=1$) can be expressed by a discrete exponential function ($\sigma_1=0$) and fixed the *p*-Ps lifetime to its average value from unconstrained fits, $\tau_1=115$ ps, and the intensity I_1 to its theoretical value $I_1/I_3=1/3$ [33,34].

A nonlinear least-squares fit of the model function, convoluted with the resolution function, to the spectra provides the following lifetime parameters as output: the intensities I_1+I_3 and I_2, the mean lifetime τ_i, and the mean dispersion σ_i of the corresponding lifetime distribution, $\alpha_i(\tau)d\tau=\alpha_i(\lambda)\lambda^2 d\tau$ ($i=2,3$).

Figure 3 shows the most important parameters of the analysis, the mean lifetime τ_3 and the width σ_3 of the lifetime distribution of *o*-Ps in DGEBA, as a function of the temperature. As can be observed, τ_3 varies between 1.3 ns at 80 K and 2.5 ns at 350 K, and σ_3 between 0.10 and 0.45 ns. In the temperature range between 80 and 325 K, σ_3 follows a linear relation with τ_3 which can be fitted approximately by $\sigma_3(\text{ns})=0.20(\pm 0.02)(\tau_3-0.5)$ or, more accurately, by $\sigma_3(\text{ns})=-0.30(\pm 0.03)+0.31(\pm 0.02)\tau_3$ for $\tau_3>1.3$ ns. For a vanishing hole size $\sigma_3\to 0$ and $\tau_3\to 0.5$ ns [see Eq. (7)] is assumed. The ratio σ_3/τ_3 at $T=T_g+50$ K is 0.18 and somewhat smaller than is usually observed for polymers, 0.25–0.35 [39–41].

The intensity I_3 of the *o*-Ps component (not shown) increases linearly from 28% at 80 K to 36% at T_g, and thereafter remains at this value. Since I_3 has no simple correspondence to the free volume, we omit a discussion of its behavior. The mean positron (e^+) lifetime τ_2 (not shown) exhibits a similar behavior to τ_3. τ_2 increases from 0.333($\pm$0.003) ns at 80 K to 0.348 ns at 255 K, and further to 0.38 at 350 K. The dispersion of the positron lifetime, σ_2, shows a weak increase, from 0.05($\pm$0.02) ns at 80 K to 0.08 ns at 350 K.

Our lifetime results for the pure epoxy resin can be compared with various studies of cured DGEBA [53–56]. These studies show that, due to increasing cross-linking during curing, the *o*-Ps lifetime, measured at room temperature, decreases from 2.3 ns to about 1.5 ns. While the glass transition shifts to temperatures between 300 and 420 K, the variation in τ_3 from below T_g to T_g+100 K is, like in the uncured state, from 1.3–1.5 ns up to 2.3–2.5 ns. Sometimes, depending on the curing agent, τ_3 values of 2.8 ns are observed.

Local free volumes

In the following section, we discuss the mean size, the width of the size distribution, and the mean number density of local free volumes (holes) probed by *o*-Ps. The usual way to calculate the mean radius $r_h(\tau_3)$ of the holes (assumed spherical) employs the equation

$$\lambda_{po} = 1/\tau_{po} = 2\ \mathrm{ns}^{-1}\left[1 - \frac{r_h}{r_h + \delta r} + \frac{1}{2\pi}\sin\left(\frac{2\pi r_h}{r_h + \delta r}\right)\right], \tag{7}$$

where $\lambda_{po}=\lambda_3=1/\tau_3$ is the mean *o*-Ps pick-off annihilation rate. This equation comes from a semiempirical model [30] which assumes that *o*-Ps is localized in an infinitely high potential well with the radius $r_h+\delta r$, where r_h is the hole radius and the empirically determined $\delta r=1.66$ Å describes the penetration of the Ps wave function into the hole walls [31,32]. The relation $\lambda_{po}=1/\tau_{po}=1/\tau_3$ is based on the assumption that spin conversion and chemical quenching of *o*-Ps are negligible. The mean hole volume is then usually calculated from $v_h(\tau_3)=(4/3)\pi r_h^3(\tau_3)$.

Since λ_{po} and, therefore, τ_3 follow a distribution, we have estimated the mean hole volume as the mass center of the hole size distribution. The radius probability distribution $n(r_h)$ can be calculated from $n(r_h)=-\alpha_3(\lambda)d\lambda/dr_h$ [37,38],

$$n(r_h) = -2\delta r\{\cos[2\pi r_h/(r_h+\delta r)] - 1\}\alpha_3(\lambda)/(r_h+\delta r)^2, \tag{8}$$

where $\alpha_3(\lambda)$ is the *o*-Ps annihilation rate distribution. The volume-weighted hole size distribution follows from $g(v_h)=n(r_h)/4\pi r_h^2$ and the number-weighted hole size distribution from $g_n(v_h)=g(v_h)/v_h$. The mean and the variance of $g_n(v_h)$, $\langle v_h\rangle$ and σ_h^2, were calculated numerically as first and second moments of this distribution. The "modified" distribution $g_n^*(v_h)=g_n(v_h)/v_h$ discussed previously by us [40,41] has, due to the small dispersion σ_h in the case of DGEBA, only slightly smaller mean values $\langle v_h\rangle^*$ than $g_n(v_h)$. However, the statistical scatter of the calculated mean volume $\langle v_h\rangle^*$ is distinctly larger than of $\langle v_h\rangle$. Therefore, we go on without discussion of these values. More details about the calculation can be found in our previous papers [39–41].

Figure 4 shows plots of the hole size distribution $g_n(v_h)$ calculated from data in the temperature range below 320 K. In Fig. 5, the mean hole volume $\langle v_h\rangle$ and the corresponding mean hole volume dispersions σ_h are displayed. $\langle v_h\rangle$ varies between ~35 Å^3 at 80 K and ~140 Å^3 at 340 K. Below T_g, *o*-Ps atoms are trapped in local free volumes within the glassy matrix and the *o*-Ps lifetime and the calculated hole size mirror the mean size of more or less static holes. The value of σ_h shows the distribution in the sizes (and shapes) of the static holes. The slight increase of $\langle v_h\rangle$ with temperature comes from the thermal expansion of free volume in the glass due to the anharmonicity of molecular vibrations and possibly from local motions in the vicinity of the holes.

In the state $T>T_g$, the structural mobilities increase rapidly in frequency [45] and amplitude [57–59], which leads to a steep rise in $\langle v_h\rangle$ and σ_h with the temperature. As already mentioned, provided the structural relaxation times are larger than the *o*-Ps lifetime, $\langle v_h\rangle$ represents the mean and σ_h the mean dispersion of the volume of holes whose size and shape fluctuate now in space and time. The intersection of the straight lines fitted to the $\langle v_h\rangle$ data of the low- and high-temperature regions determines the volumetric glass-transition temperature of $T_{gv}=T_g(\langle v_h\rangle)=260\pm4$ K, which is close to $T_g=255$ K estimated from calorimetry. The temperature where the free volume linearly extrapolated from the region above the glass transition goes to zero is estimated to be $T_{0v}=T_0(\langle v_h\rangle)=216\pm5$ K.

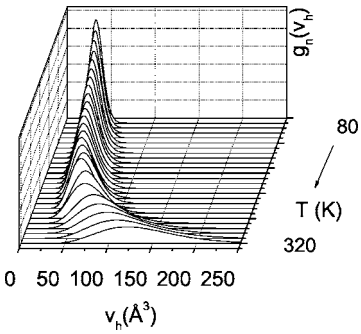

FIG. 4. Number-weighted size distribution $g_n(v_h)$ of free-volume holes in DGEBA as a function of temperature T between 80 and 320 K in steps of 10 K. The curves are normalized to the same area.

The mean hole size dispersion σ_h shows a similar glass-transition behavior to $\langle v_h\rangle$, $T_{g\sigma}=T_g(\sigma_h)=T_{gv}$. The temperature where σ_h when linearly extrapolated to lower temperatures goes to zero differs, however, from that estimated from $\langle v_h\rangle$, $T_{0\sigma}=T_0(\sigma_h)=233\pm7$ K. That is the reason that we distinguish characteristic temperatures estimated from $\langle v_h\rangle$ from those from σ_h.

At a temperature of $T_{kv}=T_k(\langle v_h\rangle)=T_g+80$ K$=340\pm5$ K (the $\langle v_h\rangle$ "knee," $T_{kv}/T_g=1.31$), the mean hole volume $\langle v_h\rangle$ levels off. We attribute this effect to structural motions; at T_{kv}

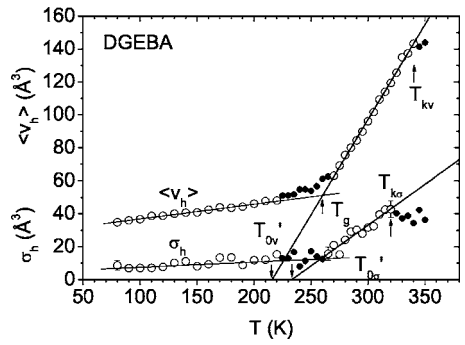

FIG. 5. The mean hole volume, $\langle v_h\rangle$, and the mean hole volume dispersion, σ_h, calculated from the number-weighted hole volume distribution $g_n(v_h)$ as a function of the temperature T for DGEBA. The lines are linear fits to the data represented by open symbols. $T_g=T_{gv}$ and T'_{0v} indicate the volumetric glass transition and the temperature where the hole volume linearly extrapolated from $T>T_g$ disappears. The extrapolated σ_h disappears at $T'_{0\sigma}$. T_{kv} and $T_{k\sigma}$ indicate the "knee" temperatures of $\langle v_h\rangle$ and σ_h, respectively (see text).

their frequencies υ come into the order of magnitude of $1/\tau_3$. As long as the structural relaxation times are significantly larger than its mean lifetime, *o*-Ps makes "snapshots" of the free volume microstructure at the moment of annihilation and τ_3 and σ_3 mirror the fluctuations of holes sizes and shapes in space and time like a quasistatic hole size distribution. For structural relaxation times of the magnitude of τ_3, the hole walls are likely to move during the life of *o*-Ps, which effectively reduces the empty space inside the holes probed by *o*-Ps. This decrease may approximately compensate for the increase in the true hole size due to increasing temperature as expected from the thermal expansion of the specific free volume.

As an appropriate scale to look to this problem, we take the value $2\upsilon\tau_3$, where υ is the frequency (in s^{-1}) of the structural relaxation. From the frequency data of Corezzi *et al.* [45], we calculated that this value is $2\tau_3\upsilon=2$ at $T=348$ K, 1 at 337 K, and 0.2 at 317 K. For a correct mirroring of the hole sizes by the *o*-Ps annihilation, the "exposure" time should be $\tau_3<1/(2\upsilon)$ or, equivalently, $2\tau_3\upsilon<1$. Recently, it was shown by Ngai *et al.* [59] for low-molecular liquids that the mean-square atomic displacement of structural relaxations with time scales shorter than 0.66 ns increases strongly at a temperature which agrees with the T_k in the *o*-Ps lifetime τ_3 (denoted by the authors as T_r).

While the knee in $\langle v_h\rangle$ is well established, the leveling-off or decrease of σ_h was recently observed for the first time by some of us [40]. From the current work, it becomes clear now that the "knee" in σ_h may appear earlier than in $\langle v_h\rangle$. We estimated $T_{k\sigma}=T_k(\sigma_h)=T_g+60$ K$=320\pm5$ K, $T_{k\sigma}/T_g=1.23$. We will show later that the appearance of the "knee" in σ_h has reasons different from that of the "knee" in $\langle v_h\rangle$ and that important aspects of the polymer dynamics and their heterogeneity appear behind the behavior of σ_h.

An estimate of the hole density may be obtained by comparing PALS and PVT experiments. The mean number of holes per mass unit, N_h', may be determined from one of the relations [60]

$$V_f = N_h'\langle v_h\rangle, \tag{9}$$

$$V = V_{\mathrm{occ}} + N_h'\langle v_h\rangle. \tag{10}$$

Equation (9) assumes that *o*-Ps detects the same hole free volume V_f as estimated from the S-S eos analysis of PVT data, $V_f=hV$, while Eq. (10) may be considered as an empirical, model-free, relation.

The plot of V_f versus $\langle v_h\rangle$ of data from the temperature range between T_g(PALS)$+10$ K$=270$ K and $T_{kv}=340$ K is linear with a constant slope of $dV_f/d\langle v_h\rangle=0.522(\pm0.02)\times10^{21}$ g^{-1} and an intercept with the y axis of $V_{f0}=0.0035\pm0.0008$ cm^3/g. Since $V_{f0}\approx0$, we constrained the final fit to pass zero and got $N_h'=dV_f/d\langle v_h\rangle=0.561(\pm0.01)\times10^{21}$ g^{-1}. The plot of V versus $\langle v_h\rangle$ delivers $dV/d\langle v_h\rangle=0.549(\pm0.01)\times10^{21}$ g^{-1} and $(V_{\mathrm{occ}}+V_{f0})=0.8065\pm0.001$ cm^3/g, which is slightly larger than $V_{\mathrm{occ}}=0.8004\pm0.001$ cm^3/g obtained from the S-S analysis for 300 K and ambient pressure. The value of $N_h'=0.56(\pm0.02)\times10^{21}$ g^{-1} corresponds to a volume-related hole density of $N_h=N_h'\rho=0.65(\pm0.02)$ nm^{-3} ($T=300$ K, $\rho=1/V$) and to a volume which contains one hole of $1/N_h=1.54$ nm^3.

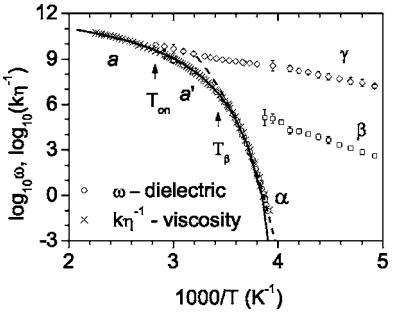

FIG. 6. Relaxation map (Arrhenius plot) of DGEBA, showing the primary (α,a',a) relaxation process from dielectric relaxation [circles, frequencies ω (rad s^{-1})$=1/\tau_{\max}$] and from the rescaled inverse viscosity, $k\eta^{-1}$ ($\log_{10}k=8.4$ and η in Pa s, crosses), and the secondary processes β (squares) and γ (diamonds, both from dielectric relaxation, all redrawn from Corezzi *et al.* [45], Fig. 7) as a function of the reciprocal temperature $1/T$. The solid line is a fit of Eq. (3) to the primary relaxation data from the temperature range between $T_\beta=285$ and 443 K (a' and a process), the dashed line fits the data from the range below 270 K (α process).

Free volume and dynamics of DGEBA: Temperature dependency

In the following section, we attempt to analyze the dynamic properties of DGEBA, as shown by dielectric relaxation and viscosity data of Corezzi *et al.* [45], in terms of the free volume model discussed in the Introduction. The relaxation map (i.e., Arrhenius plots of the characteristic circular frequencies $\omega_i=1/\tau_{i,\max}=2\pi\upsilon_{i,\max}$, $\upsilon_{i,\max}$ is the frequency in s^{-1}, of maximum in the dielectric loss ε'' of the ith process at a given temperature T and pressure P) of DGEBA shows three processes which are plotted in Fig. 6 (redrawn from Fig. 7 in Ref. [45]). The major or primary process is attributed to the structural relaxation (dynamic glass transition) and shows VFT behavior with different parameters of Eq. (3) in the temperature ranges below 285 K (α process), between 285 and 351 K (a' process), and above 351 K (a process). Two secondary processes, β and γ, appear which also persist below T_g. The β relaxation separates at the crossover temperature $T_\beta=285\pm3$ K from the (a',α) trace and shows Arrhenius behavior, while the γ-relaxation separates from the (a,a') trace at the onset temperature $T_{\mathrm{on}}=T_\gamma=351\pm4$ K and displays Arrhenius behavior below T_g and more complicated behavior above T_g.

A VFT fit of the α-relaxation data from the temperature range between 255 and 285 K provided the parameters of Eq. (3) $T_0=209\pm2$ K, $B=2060\pm180$ K, and $\log_{10}\omega_0=18.0\pm0.7$. From the data in the temperature range between 285 and 351 K (a'-process), the parameters $T_0=234.4\pm0.8$ K, $B=720\pm20$ K, and $\log_{10}\omega_0=14.78\pm0.09$ were estimated [45]. In addition to ω, the rescaled inverse viscosity, $k\eta^{-1}$ ($\log_{10}k=8.4$ and η in Pa s), from the temperature range between 255 and 443 K is shown. The values for T_0 and B estimated from a' dielectric relaxation agree

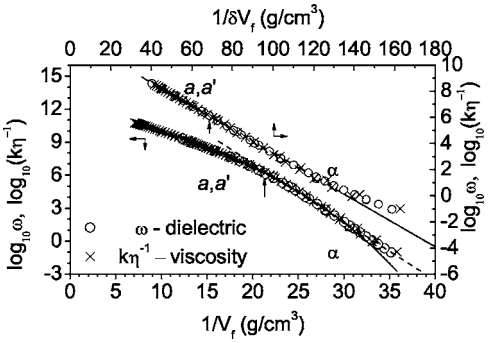

FIG. 7. "Modified" relaxation map (Cohen-Turnbull plot) of DGEBA, showing the dielectric frequencies ω (circles) and the rescaled inverse viscosity, $k\eta^{-1}$ (crosses, both data from Corezzi *et al.* [45]) of the primary (α,a',a) relaxation process, as a function of the reciprocal specific hole free volume $1/V_f$ (lower part of the figure). The data were taken from the temperature range between 255 and 443 K. The solid line is a fit of Eq. (11) to the data from the temperature range between 285 and 443 K (a' and a process, $\Delta V=0.015$ cm^3/g) and the dashed line to the data from below 270 K (α process, $\Delta V=0$). The upper part of the figure shows the plots of ω and $k\eta^{-1}$ vs the reciprocal mean fluctuation of the hole free volume $1/\delta V_f$. These data were taken from the temperature range between 255 K and $T_{k\sigma}=320$ K. The line is a linear fit to the data from above 285 K.

with the viscosity data from the whole temperature range between 285 and 443 K (a', a process).

In Fig. 7, we have shown the "modified" relaxation map. Following Eq. (1), the frequencies of the primary (structural) dielectric relaxation, $\omega=1/\tau_{\max}$, are plotted in a logarithmic scale versus the inverse free volume $1/V_f$ in the temperature range between 255 and 343 K. This presentation shown in the lower part of the figure may also be denoted as a Cohen-Turnbull (CT) plot. We will discuss the data in the upper part of the Fig. 7 in a later section. Again V_f was assumed to follow the linear relation Eq. (6), $P=0$ MPa. The parameters $T_0'=211\pm3$ K and $E_{f0}=6.09(\pm0.03)\times10^{-4}$ cm^3 g^{-1} K^{-1} were now estimated from linear fits to all of the V_f data from PVT and PALS experiments ($V_f=N_h'\langle v_h\rangle$, $N_h'=0.56\times10^{21}$ g^{-1}) in the temperature range between 270 and 440 K.

As can be observed in Fig. 7, the plots of $\log_{10}\omega$ versus $1/V_f$ are not linear but show a curvature. Generally, a linearization of the $\log_{10}\omega$ versus $1/V_f$ plots and the disappearance of relaxation, $\omega\to0$, at $T\to T_0$ can be obtained when including a term of the type $\exp[-E/R(T-T_0)]$ into the preexponential factor of Eq. (1). This term may be interpreted as a contribution of the thermal energy to the molecular motions and might have its origin in the intermolecular coupling in the development of cooperativity.

Another empirical way of linearization has been introduced by Utracki *et al.* [27,61] and was applied by some of us in a previous work [20]. The plots may be linearized when substituting $1/V_f$ by $1/(V_f-\Delta V)$ with a suitable chosen value of ΔV.

For finding the value of ΔV, we apply an idea developed by Stickel *et al.* [62] to analyze T_0 and B of Eq. (3). These authors linearized Eq. (3) by introducing the form $[d\log\omega/dT]^{-1/2}=B^{-1/2}(T-T_0)$. Analogously, we linearize

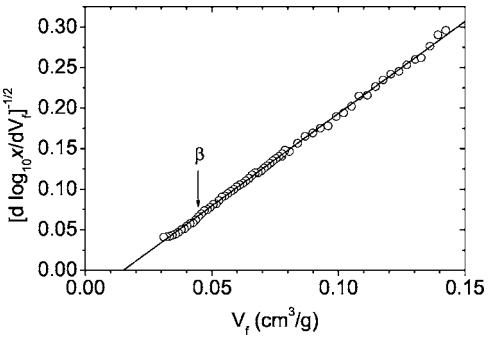

FIG. 8. Plot of $[d\log_{10}x/dV_f]^{-1/2}$ (here $x=k\eta^{-1}$, $\log_{10}k=8.4$, η in Pa s) for DGEBA vs the specific free volume V_f. The straight line is due to a linear fit to the data from above $T_\beta=285$ K.

Eq. (1) with the substitution of V_f by $(V_f-\Delta V)$,

$$\log_{10}\omega=\log_{10}C-(\gamma V_f^*/\ln 10)/(V_f-\Delta V), \tag{11}$$

by introducing the form

$$[d\log_{10}\omega/dV_f]^{-1/2}=\frac{[d\log_{10}\omega/dT]^{-1/2}}{[dV_f/dT]^{-1/2}}=\left(\frac{\gamma V_f^*}{\ln 10}\right)^{-1/2}(V_f-\Delta V). \tag{12}$$

It follows that after this transformation, the CT equation appears as a linear dependency of the left-hand side of Eq. (12) on V_f with the slope and intercept yielding the parameters γV_f^* and ΔV. We remark that in the case of a linear dependency of V_f on T, the slope $dV_f/dT=E_f=$const, $\Delta V=E_f(T_0-T_0')$, and $\Delta V=0$ for $T_0'=T_0$.

Figure 8 shows plots of $[d\log_{10}/dV_f]^{-1/2}$ versus V_f. For clarity we show here only the data derived from the rescaled inverse viscosity, however from the whole temperature range between 255 and 443 K. $[d\log_{10}\omega/dT]^{-1/2}$ was taken from the work of Corezzi *et al.* (Fig. 9b in Ref. [45]) and $[dV_f/dT]^{-1/2}$ from our work. Most of the data follow a single CT equation. The solid line in Fig. 8 shows a linear fit to the data from the temperature range above of $T_\beta=285$ K, which delivers the parameters $\gamma V_f^*=0.445(\pm0.001)$ cm^3/g and $\Delta V=0.0151\pm0.001$ cm^3/g ($r^2=0.9990$). This linear fit describes also the data down to 270 K. The data from below 270 K show a curvature and were not analyzed in this plot.

The question which now appears is the physical origin and meaning of ΔV. Recently, some of us [20] proposed that $\Delta V>0$ is an indication that it is not the entire specific hole free volume V_f, as calculated from the S-S eos, that is related to the main relaxation process via the free volume mechanism but a smaller portion, $V_f-\Delta V$. In this context, it is physically reasonable to assume that the local free volume present in monovacancies in the S-S lattice may be too small to show a liquidlike behavior and an activation energy is required for the cooperative rearranging of mers. Multivacancies may, however, show this behavior and allow a free exchange of free volume in their surroundings by thermal fluctuations, i.e., without a thermal activation in the ordinary sense. This philosophy corresponds to a two-phase model

with liquidlike and solidlike clusters of mers and is close to that of the modified free volume model of Cohen and Grest [14].

In the following, we calculate the part of the specific free volume which appears in the form of multivacancies and contains m or more (mono) vacancies. This partial volume can be written as

$$V_f^m = V_f \sum_{i=m}^{\infty} p_i, \tag{13}$$

where the quantity p_i is defined as the fraction of free volume present in agglomerates which contain i vacant lattice sites normalized here to $\Sigma p_i = 1 (i = 1 - \infty)$.

Vleeshouwers *et al.* [63] have performed Monte Carlo simulations to obtain the agglomerate size distribution as a function of the hole fraction $h(T)$ derived from the S-S eos assuming a random distribution of empty lattice cells. The MC results were represented by the empirical function

$$p_i = p_0 \exp\{-[i/l(y)]^{\beta(y)}\} \text{ for } 0.8 \leqslant y \leqslant 0.99 \text{ and } i = 1,2,3,\ldots \tag{14a}$$

$$\text{with } l(y) = 12.374 - 12.035y \tag{14b}$$

$$\text{and } \beta(y) = 0.4088 - 2.5242y + 3.1156y^2, \tag{14c}$$

where p_0 is a normalization factor, $\Sigma p_i = 1$. The equation is valid within the range $0.80 \leqslant y \leqslant 0.99$ of the occupation fraction $y = 1 - h$. Analysis shows that the distribution of Eq. (14) corresponds closely to the exponential free volume distribution derived by Cohen and Turnbull [13].

As Fig. 9 shows, the volume V_f^m decreases with increasing m and can be approximated at higher temperatures by a linear dependence on T with almost the same slopes for different m. The picture is similar to that obtained from molecular-dynamic simulations of polymer structure when scanning the empty space with probes of increasing size [64]. Our approach corresponds also to the philosophy in a later paper of Turnbull and Cohen [13], who defined the free volume by $V_f = V - V_0'$, where V_0' is considered as a temperature-independent fitting parameter of Eq. (1).

The temperature T_0' where the linearly extrapolated V_f^m disappears increases with increasing m. The comparison of V_f^m with the volume $V_f - \Delta V$, $\Delta V = 0.015$ cm^{3}g, from the CT fits shows that for the DGEBA resin the primary dielectric relaxation in the temperature range between 285 and 340 K follows the free volume theory of Cohen and Turnbull when considering that part of the free volume that occurs as vacancy agglomerates with (on the average) ~ 1.5 (corresponding to 1.5×38 Å$^3 = 57$ Å^3) or more vacancies in an agglomerate. The same is true for the viscosity in the temperature range up to 440 K. For PVAc, some of us estimated that a minimum agglomerate size of 3 (corresponding to 3×46 Å$^3 = 138$ Å^3) vacancies is required to describe the primary relaxation process [20].

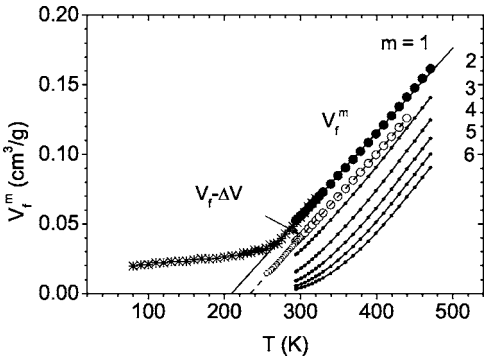

FIG. 9. Specific free volume V_f^m of agglomerates containing not less than m empty cells (vacancies) of the S-S lattice within one agglomerate ($m = 1$, filled circles; $m = 2,3,4,5,6$ lines with dots, all for $P = 0.1$ MPa) in comparison with the quantity $V_f - \Delta V$, calculated with $\Delta V = 0.015$ cm^3/g (large empty circles) and directly from the relaxations frequencies by inverting Eq. (1) (small empty circles). The crosses are calculated from the PALS data via $V_f = N_h' \langle v_h \rangle$, $N_h' = 0.57 \times 10^{21}$ g^{-1}. The solid lines represent a linear fit to the $V_f(m=1)$ and PALS data in the temperature range between 270 and 440 K; the dashed line shows the linear extrapolation of the $(V_f - \Delta V)$ data.

Free volume and dynamics of DGEBA: Pressure dependency

Now we discuss the pressure dependency of the dielectric relaxation in DGEBA in terms of the Cohen-Turnbull free volume model. Corezzi *et al.* [45] found that the Cohen-Grest free volume theory of mobility [14], which is an extension of the Cohen-Turnbull model, can describe the temperature dependency of primary relaxation in DGEBA in the whole range of temperatures. This is not surprising because the Cohen-Grest equation has one more parameter than Eq. (1). Moreover, such fits do not represent an independent determination of the free volume. The pressure dependency of the primary relaxation, however, did not follow the Cohen-Grest equation.

From a CT fit to the primary relaxation data of Corezzi *et al.* [45] (not shown), we obtained, when including all data in the pressure range between 0.1 and 200 MPa into the fit, the parameters $\Delta V = 0.013 \pm 0.003$ cm^3/g, $\log_{10} C = 11.3 \pm 0.1$, and $\gamma V_f^* = 0.39 \pm 0.01$ cm^3/g ($r^2 = 0.9998$). These parameters are close to those obtained previously from the temperature dependency of the (a', a) relaxation. The parameters depend, however, distinctly on the range of pressures included into the fit. This may be attributed to the beginning of the liquid-glass transition at higher pressures.

We remark at this point that the pressure dependency of the fragility $m = -d(\log_{10} \omega)/d(T_g/T)_{T=T_g} = (B/\ln 10) T_g/(T_g - T_0)^2$ [do not mix this m with the m in Eqs. (13)] of the glass forming liquid can be expressed by the pressure dependence of B, T_g, and T_0. The pressure dependence of T_g and T_0 estimated from dielectric relaxation experiments [15,45,46], $dT_g/dP = 0.137$ K/MPa and $dT_0/dP = 0.112$ K/MPa, is indicated in Fig. 2. With $B = \gamma V_f^*/E_f$ [$E_f = \alpha_f V_{fg}$, $V_{fg} = V_f(T_g)$] and assuming $T_0' = T_0$, we obtain the relation $m = (1/\ln 10) \times (\gamma V_f^*/V_{fg}) T_g \alpha_f$. Recently, it has been shown for some low molecular liquids that m varies linearly with the coefficient

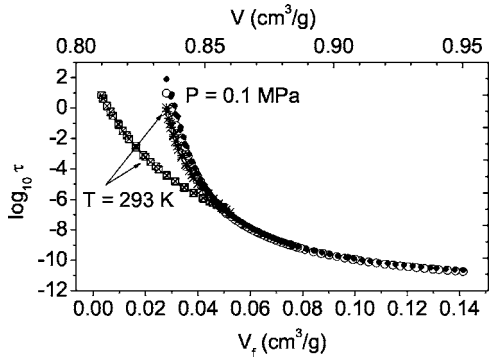

FIG. 10. Comparison of isothermal (crosses and cross-centered squares, from Ref. [47]) and isobaric (open and filled circles, from Ref. [45]) dependencies of relaxation times $\tau=1/\omega$ (in seconds) plotted as function of the free volume $V_f(T,P)$ (bottom x axis, crosses and open circles) and of the total volume $V(T,P)$ (top x axis, cross-centered squares and filled circles) for DGEBA. For clarity, we have shown for the isobars only the rescaled viscosity ($\tau \equiv \mathrm{k}^{-1}\eta$).

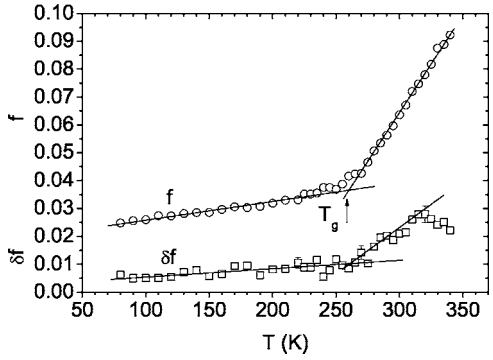

FIG. 11. Mean fractional free volume, $f=\langle V_f\rangle/\langle V\rangle=N_h'\rho\langle v_h\rangle$, and root-mean-square fluctuation of the fractional free volume, $\delta f=(\langle \delta V_f^2\rangle/\langle V\rangle^2)^{1/2}=N_h'\rho\sigma_h$, derived from the PALS data of DGEBA.

of thermal expansion of the free volume, α_f [65]. For PVAc [20] we have previously determined that γV_f^* is independent of the pressure so that the pressure dependency of $B=\gamma V_f^*/E_f$ comes in that case exclusively from $E_f(P)$.

For comparison of the data from pressure experiments with those from temperature experiments, we use a presentation frequently shown in the literature [15–17]. Figure 10 displays plots of isobaric and isothermal relaxation times, $\tau(T,P)=1/\omega(T,P)$, versus the free volume $V_f(T,P)$ and the same plots versus the total volume $V(T,P)$. The V_f and V axis were scaled so that the first and the last data point of the isobaric data match. These isobaric data agree almost perfectly over the whole range of volumes (temperatures). The remaining small discrepancy between the log τ versus V_f and versus V plots is due to the slight variation of V_{occ} ($V_f=V-V_{\mathrm{occ}}$) with the temperature.

The isothermal plots of log τ versus V_f and versus V clearly disagree, however. The same is true for isothermal and isobaric dependencies of log τ when plotted versus V. From this kind of discrepancy, the relative contributions of temperature and density to the relaxation rate have been concluded [15–17]. However, as discussed previously, this discrepancy largely comes from the compressibility of the occupied volume. When plotting the data versus $V_f=V-V_{\mathrm{occ}}$, most of the discrepancy disappears. The remaining differences indicate deviations from the free-volume model (as $\Delta V\neq 0$ shows) and the role of temperature in the relaxation process. Further research may quantify the contributions of *free* volume and temperature as controlling variables of the structural relaxation process.

Thermal fluctuations and hole size distribution

Thermal fluctuations cause a fluctuation in the size of a subvolume which contains a fixed number of molecules. From standard thermodynamics, the mean-square fluctuation of this subvolume $\langle \delta V^2\rangle=\langle (V-\langle V_{\mathrm{SV}}\rangle)^2\rangle=k_BT\,\kappa\langle V_{\mathrm{SV}}\rangle$ follows where $\langle V_{\mathrm{SV}}\rangle$ is its mean and all other values have the usual meaning [66]. Assuming that the fluctuations in the free and occupied volume are independent, $\langle \delta V^2\rangle=\langle \delta V_f^2\rangle+\langle \delta V_{\mathrm{occ}}^2\rangle$, one obtains for the mean-square fluctuation of the free volume

$$\langle \delta V_f^2\rangle = k_BT\kappa_f\langle V_f\rangle = k_BT\kappa_f^*\langle V_{\mathrm{SV}}\rangle, \tag{15}$$

where $\langle V_f\rangle$ is the mean free volume within the subvolume $\langle V_{\mathrm{SV}}\rangle$. $\kappa_f=-(1/V_f)(dV_f/dP)_T$ is the mean compressibility of the free volume and $\kappa_f^*=-(1/V)(dV_f/dP)_T=h\kappa_f$ is the corresponding fractional compressibility. κ_f^* is frequently approximated by the change in the compressibilities at T_g, $(\kappa_f^*)\approx\Delta\kappa=\kappa_{\mathrm{liquid}}-\kappa_{\mathrm{glass}}$. In our case, however, we can calculate the exact value of $\kappa_f^*(T)$ from our free volume data.

Volume fluctuations occur on many time scales, including very fast fluctuations associated with vibrational motions. We are interested in slow fluctuations which are related to the structural relaxation and determine the compressibility κ_f^*. We assume that PALS mirrors such fluctuations in the free volume; its mean is $\langle V_f\rangle=(N_h'\rho\langle V_{\mathrm{SV}}\rangle)\langle v_h\rangle=(N_h\langle V_{\mathrm{SV}}\rangle)\times\langle v_h\rangle$, like a quasistatic hole size distribution as long as the structural relaxation time is larger than the o-Ps lifetime (i.e., at temperatures below T_{kv}). From this it follows that the mean-square fluctuation in the free volume can be estimated from the PALS experiments via [39–41]

$$\langle \delta V_f^2\rangle = (N_h'\rho\langle V_{\mathrm{SV}}\rangle)^2\langle \delta v_h^2\rangle = (N_h\langle V_{\mathrm{SV}}\rangle)^2\sigma_h^2, \tag{16}$$

where ρ is the mass density and $\langle \delta v_h^2\rangle=\langle (v_h-\langle v_h\rangle)^2\rangle$ is the mean-square fluctuation of the hole volume, which we have estimated as variance $\sigma_h^2=\langle \delta v_h^2\rangle$ of the hole size distribution $g_n(v_h)$ and shown in Fig. 5 as mean dispersion σ_h. We have assumed in Eq. (16) that the holes detected by PALS fluctuate independently in size and number, and that the fluctuations in number are negligible, $\delta N_h'=0$ and $\langle N_h'\rangle=N_h'$. This assumption is justified by the temperature independency of N_h'. Figure 11 shows the root-mean-square fluctuation of the fractional free volume, $\delta f=\langle \delta V_f^2\rangle^{1/2}/\langle V\rangle=N_h'\rho\sigma_h=N_h\sigma_h$, in comparison with the mean fractional free volume calculated via $f=\langle V_f\rangle/\langle V\rangle=N_h'\rho\langle v_h\rangle=N_h\langle v_h\rangle$. $\rho=1/V$ was calculated using a quadratic fit function for V and assuming that V decreases below T_g linearly with a coefficient of $\alpha_g=2\times10^{-4}\ \mathrm{K}^{-1}$. As can be observed, δf varies from 0.5% at

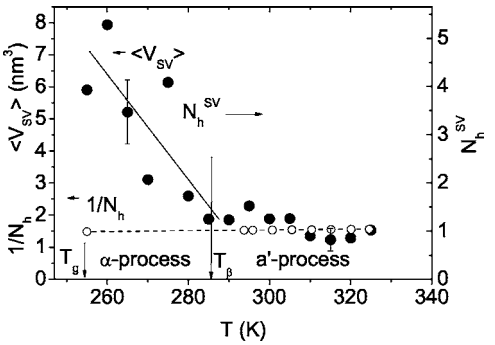

FIG. 12. The volume of the smallest representative freely fluctuating subsystem, $\langle V_{SV}\rangle$ (filled circles), as estimated from PALS and PVT data of DGEBA. For comparison the volume which contains one *o*-Ps hole, $1/N_h$ (empty circles), is shown. The right-hand *y* scale shows the number of *o*-Ps holes in a subvolume, $N_h^{SV}=\langle V_{SV}\rangle N_h$ using the approximation $1/N_h=1.5$ nm^3 (the same data points as for $\langle V_{SV}\rangle$). The lines are a guide for the eyes.

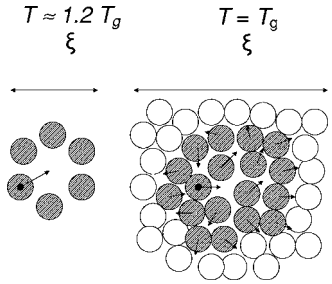

FIG. 13. Schematic illustration of the spatial structure of the smallest representative subvolume which is derived from the volume fluctuations detected by PALS, $\langle V_{VS}\rangle=\xi^3$, at high temperatures ($T\approx 1.2\ T_g$, the *a* process) and at T_g (the cooperative α process) and its relation to particle mobilities. Shown are empty spaces (represented by empty areas) which constitute the fluctuating free volume and particles (spheres). The larger empty spaces are probed by *o*-Ps (holes). ⊙ is a particle considered at its movement near a hole, ● are particles with higher mobility, and ◯ are particles with lower mobility. The arrows indicate the possible movement of particles.

80 K to 1% at T_g and further to 2.8% at 320 K. f increases from 2.5% to 3.5% and finally to 9%. We remark that f has the same meaning as h calculated from the S-S eos. The relative fluctuation $\delta f/f=\sigma_h/\langle v_h\rangle$ amounts to 0.20 at low and 0.35 at higher (320 K) temperatures. The leveling-off of δf above $T=320$ K is caused by the leveling-off of σ_h and will be discussed below.

From combining Eqs. (15) and (16), we obtain

$$\langle V_{SV}\rangle = k_B T\kappa_f^*/N_h'^2\rho^2\sigma_h^2 = k_B T\kappa_f^*/\delta f^2, \tag{17}$$

where $\delta f^2=\langle \delta V_f^2\rangle/\langle V_{SV}\rangle^2=N_h^2\sigma_h^2$. We note that the corresponding formula for fluctuations in the (total) mass density, $\delta\rho$, is $\langle V_{SV}\rangle=k_B T\ \kappa/(\langle\delta\rho^2\rangle/\rho^2)$. Employing small-angle x-ray scattering (SAXS), the value $\langle\delta\rho^2\rangle/\rho$ can be derived from the intensity $I(0)$ of the scattering curve [67,68]. From this value, the compressibility κ but not the subvolume $\langle V_{SV}\rangle$ can be calculated.

Equation (17) involves three assumptions. (i) Intensive quantities of the subsystem are identical with the corresponding macroscopic quantities and extensive quantities follow linearly the size of the subsystem. (ii) The spatial free volume fluctuations detected at a macroscopic sample via *o*-Ps annihilation "snapshots" are representative for fluctuations of the free volume of one average subsystem. (iii) The thermal fluctuations are dominated by the (slow) structural relaxation. From these assumptions it follows that $\langle V_{SV}\rangle$ can be considered as the mean volume of the smallest representative freely fluctuating subsystem related to structural relaxation. (Compare the gedanken experiment of Donth [1,69] for the estimation of the size of the subvolume from heat capacity spectroscopy data.)

The subvolume defined by Eq. (17) has a similar meaning to the volume of a cooperatively rearranging region (CRR) of the Adam-Gibbs theory [9]. The CRR is considered as the smallest independent distinguishable (representative) subsystem for the structural (α) relaxation.

Figure 12 shows the behavior of $\langle V_{SV}\rangle$ calculated from Eq. (17) and taking σ_h and N_h' from the PALS and κ_f^* and ρ from the PVT experiments. $1/N_h$ shows the volume which contains one hole. To calculate $\langle V_{SV}\rangle$ for the temperature range between 293 K and T_g, we have extrapolated κ_f^* and $V=1/\rho$ by using quadratic functions. $\langle V_{SV}\rangle$ varies from $\sim$7 nm^3 at $T_g=255$ K to 2.3 nm^3 at 293 K and further to $\sim$1 nm^3 at temperatures above 310 K. We have reported a similar variation of $\langle V_{SV}\rangle$, which was estimated for the first time from PALS data, recently for two fluoroelastomers [40,41]. $1/N_h$ is almost constant at $\sim$1.5 nm^3. The value of $\langle V_{SV}\rangle$ at T_g corresponds to a characteristic length of $\xi=\langle V_{SV}\rangle^{1/3}=1.9$ nm. In the literature, characteristic lengths for the dynamic heterogeneity of structural (α) relaxation at T_g in different glass formers of $\xi_\alpha=1-3.5$ nm are estimated from dynamic heat capacity data [1,70–73]. Domains of similar size were detected in multidimensional nuclear magnetic resonance (NMR) experiments by Spiess and collaborators [74]. ξ_α decreases with increasing temperature and the dynamic heterogeneity disappears at a critical temperature above T_β [1].

The variation in $\langle V_{SV}\rangle$ is mainly controlled by the variation in $1/\sigma_h^2$ [Eq. (17)]. Since σ_h varies as $\sim(T-T_{0\sigma}')$ ($T_{0\sigma}'=233$ K), $\langle V_{SV}\rangle$ should vary as $\sim 1/(T-T_{0\sigma}')^2$. This result agrees with Donth's findings $V_\alpha=\xi_\alpha^3\sim 1/(T-T_0)^2$, where T_0 is the Vogel temperature of the structural relaxation [1].

In the following part, we attempt to correlate the spatial structure as concluded from PALS for higher and lower temperatures with the known mobility pattern of glass-forming liquids [1]. Figure 13 shows a scheme of our model. The fluctuating subvolume at T_g (here 255 K) is large and contains many particles (molecules or monomeric units) in areas with different packing densities. There are many small empty spaces between the particles; the larger ones are detected by *o*-Ps as several (small) holes. Since the empty spaces and holes are small, the considered particle can only move when a number of particles in its surroundings (which form a cage for this particle) cooperatively rearrange. On the other hand, the appearance of *several small* holes (and further smaller

empty spaces) *allows* a cooperative rearrangement of particles. A spatial structure like this is expected to be characteristic of the structural relaxation in "cold" liquids (cooperative α process) [1]. The estimated parameters of the subvolume at T_g for DGEBA are $\xi \approx 1.9$ nm, $\langle V_{VS}\rangle \approx 7$ nm^3, $\langle 2r_h\rangle = 0.48$ nm, $\langle v_h\rangle = 0.06$ nm^3, $f=h=0.039$ (volume fraction of holes), and $f_{total} \approx 0.35$ [$f_{total}=(V-V_W)/V$ is the total free volume fraction, V_W is the van der Waals volume]. In the mean, a number of $N_h^{SV}=\langle V_{VS}\rangle N_h'\rho=\langle V_{VS}\rangle N_h=4$ to 5 (o-Ps) holes occupy one subvolume.

At higher temperatures above the onset of the β process, say at $T=1.2$, $T_g=310$ K, the fluctuating subvolume contains only *one* (but *large*) (o-Ps) hole. All particles have such a hole into which they may jump in their next surroundings. Therefore, all particles are dynamically equivalent and the dynamic heterogeneity disappears. This situation is considered to be characteristic of structural relaxations in the "hot" liquid (a' and a process) [1]. The estimated parameters of the subvolume at $T=1.2\ T_g$ for DGEBA are $\xi \approx 1.0$ nm, $\langle V_{VS}\rangle \approx 1$ nm^3, $\langle 2r_h\rangle = 0.60$ nm, $\langle v_h\rangle = 0.11$ nm^3, $N_h^{SV} \approx 1$, $f=h=0.072$, $f_{total} \approx 0.38$.

As we have found, the primary α and a',a relaxations are associated with a thermal expansion of o-Ps holes (agglomerates of S-S lattice vacancies) and a constant specific hole number while the representative subvolume shrinks from a larger size, which contains several holes, to the minimum, which contains just one hole. The conclusions from our experiments illustrated in Fig. 13 correspond closely to the description of an island of increased free volume and increased mobility which is located in the inner part of a CRR, as described by Donth [1] and characterized as Glarum-Levy defect [75]. There seems to exist, however, no one-to-one correspondence of a (*single*) hole and the Glarum-Levy defect, at least at temperatures near T_g.

The secondary β relaxation (Johari-Goldstein process) is considered as a local process [1,2] which occurs in the vicinity of empty spaces or holes. At temperatures below T_g where the β relaxation can be observed in dielectric relaxation experiments (Fig. 6), usually no or only a weak thermal expansion of o-Ps holes is observed (Fig. 5). We expect that the volumetric inactivity or weakness of the β (Johari-Goldstein) process is related to its noncooperative, local, nature. It is known that the cooperative α process shows a caloric activity which decreases with increasing temperature up to a low constant value which is characteristic for the high-temperature a process. The β (Johari-Goldstein) relaxation, however, has no detectable caloric activity [1].

Our values for $\langle V_{SV}\rangle$ can be compared with the volume V_α of a CRR calculated from heat capacity spectroscopy data of the DGEBA [45] using the fluctuation approach to the glass transition by Donth [1]. This approach starts from the nonconventional von Laue approach [76] in the form of the Landau-Lifshitz fluctuation formula [66] $\langle \delta T^2\rangle = k_B T^2/C_v$ and leads with the specific heat of a CRR expressed by $C_v = c_v \rho \langle V_{SV}\rangle$ to the equation

$$V_\alpha = \xi_\alpha{}^3 = (k_B/\rho)\Delta(1/c_v)/(\langle \delta T^2\rangle/T^2), \qquad (18)$$

where $\langle \delta T^2\rangle$ is the mean-square fluctuation in the temperature of a CRR, functional of the dynamic glass transition [i.e., structural ($\alpha-$) relaxation]. The approximations $c_v \approx c_p$ for the mean specific heat and $\Delta(1/c_p) = 1/c_p(\text{glassy zone}) - 1/c_p(\text{flow zone})$, the step height of the reciprocal mean specific heat at constant pressure at glass transition, are used. The analysis of Corezzi *et al.* [45], who determined $\delta T = (\langle \delta T^2\rangle)^{0.5}$ as the mean dispersion in the imaginary part of the dynamic heat capacity, showed that the cooperativity N_α (defined as the number of molecules or monomeric units in the subvolume V_α) varied from ~60 at 260 K to 16 at 275 K and to ~1 at 310 K (extrapolated, Fig. 10 in Ref. [45]). This corresponds to a change in the volume of the CRR from 32 to 8 cm^3 and further to 0.5 nm^3.

Compared with these caloric data, the values of (V_{SV}) estimated from the PALS data are smaller at T_g and larger at $T \approx 1.2T_g$. Possible sources for this difference may be the limited resolution of PALS with respect to the width of the lifetime distribution or the assumed shape of this distribution. Due to the finite internal resolution of measurements and data analysis, we may expect an overestimation of small σ_3 values. If σ_3 is rather large, the background in the lifetime spectra may cause an underestimation of this value. We should also take into account, however, that even the caloric data are not very accurate and typical errors in the estimation of N_α are estimated to lie between 50% and 200%.

Another, more fundamental reason for the differences between the estimates from PALS and the dynamic heat capacity could come from the different physical quantities detected in both methods and/or the different underlying thermodynamics. We remark that Eq. (17) is strictly valid only if the smallest representative subvolume $\langle V_{SV}\rangle$ contains just one hole (or if all holes within the subvolume fluctuate coherently and in phase, which is highly unlikely). Figure 13 shows, however, that at T_g several holes occupy the subvolume $\langle V_{SV}\rangle$. These holes may fluctuate at a given moment with a different sign of $(v_h - \langle v_h\rangle)$, which leads to an overestimation of $\langle \delta V_f^2\rangle$ when calculated from Eq. (16). The subvolume $\langle V_{SV}\rangle$ calculated from Eq. (17) must then be considered as a lower limit of the true value.

We also point out that from the point of view of PALS, the smallest representative subvolume that can occur at higher temperatures ($T \approx 1.2T_g$) must consist of a single hole surrounded by a wall or shell of molecular thickness. When modeling the spatial structure by a periodic lattice with 12 next neighbors and assuming that the hole occupies a lattice site, 3 of the 12 next neighbors of the hole belong to this hole. Thus, the smallest representative subvolume for vanishing dynamic heterogeneity contains the hole and approximately three particles (molecules or monomeric units). Since at a temperature of $1.2T_g$ the hole diameter amounts to 0.6 nm, the (minimum) characteristic length scale of the spatial heterogeneity should not differ much from $\xi \approx 1.2$ nm ($\langle V_{SV}\rangle \approx 1.5$ cm^3). This is in perfect agreement with our data shown in Fig. 13 but larger than $\xi_\alpha = 0.8$ nm($\langle V_{SV}\rangle = \xi_\alpha^3 \approx 0.5$ nm^3) estimated from the dynamic heat capacity [45].

Apparently, the characteristic length scale of the dynamic heterogeneity ξ detected by PALS as a spatial heterogeneity caused by thermal volume fluctuations has a meaning that differs from that of the characteristic length scale ξ_α of dy-

namic heterogeneity as obtained from the dynamic heat capacity using Eq. (18). Further research may clear up the important question of accuracy and comparability of both methods.

Finally, in this section, we recall that the Vogel temperature $T_0(a')=234.4\pm0.8$ K of the high-temperature ($T>T_\beta=285$ K) structural (a',a) relaxation [45] agrees with the temperature $T'_{0\sigma}=233\pm7$ K where the hole size dispersion σ_h extrapolated linearly to lower values (Fig. 5) vanishes. At the same temperature, the mean fluctuation in the specific free volume calculated from $\delta V_f=N'_h\sigma_h$ (N'_h=const) goes to zero, while the mean free volume $V_f=N'_h\langle v_h\rangle$ vanishes at a lower temperature of $T'_{0v}=216\pm5$ K.

The behavior of V_f and δV_f corresponds to the temperature dependency of an external free volume and an internal fluctuating free volume as described in the free volume theory of Donth [1,77]. This theory predicts that the internal fluctuating free volume controls the high-temperature (a') relaxation until its exhausting at a temperature $T_E\approx T_\beta$. Exhausting stops the original, high-temperature VFT (or WLF) equation for the a' process and leads to its substitution by a more effective, low-temperature VFT equation (α process) characterized by a lower Vogel temperature $T_0(\alpha)<T_0(a')$.

Inspired by Donth's theory, we employ again the Cohen-Turnbull free volume formula Eq. (1) but assume that the dynamics is controlled by the free volume fluctuations. Equation (1) reads then like

$$\omega = C\exp(-\delta V_f^*/\delta V_f). \tag{19}$$

Figure 7 shows in its upper part the plot of $\log\omega$ versus $1/\delta V_f$, where δV_f was interpolated using the relation $\delta V_f=N'_h e_\sigma\,(T-T'_{0\sigma})$ ($N'_h=0.56\times10^{21}$ g^{-1}, $e_\sigma=0.495$ Å^3/K, $T'_{0\sigma}=233$ K, compare Fig. 5). The plot is linear, i.e., follows the Eq. (19) in the whole temperature range above 265 K. The analyzed parameters are $\log_{10}C=12.27(\pm0.01)$, which is in agreement with the VFT analysis of Corezzi *et al.* [45] and $\delta V_f^*=0.2076(\pm0.001)$ cm^3/g. This interesting finding and its relation to the free volume theory of Donth will be the subject of further research.

Dispersion in dielectric loss and hole size distribution

Finally, we discuss the interrelation between the dispersion in the dielectric loss function $\varepsilon''(\omega)$ and the dispersions in the hole sizes $g_n(v_h)$. When applying Eq. (1), $\ln\omega=\ln C-(\gamma V^*/N'_h v_h)$, in a local approximation we may establish the following relation for the mean logarithmic dispersion (square root of variance) of the frequency distribution curve $\varepsilon''(\ln\omega)$:

$$\delta\ln\omega=(\gamma V^*/N'_h)\,\delta(1/v_h). \tag{20}$$

Here $\delta(1/v_h)$ is the square root of the variance of the hole size distribution curve in reciprocal coordinates, $g_n(1/v_h)$. $\delta(1/v_h)$ can be approximated by $\delta(1/v_h)=1/v_{hm}-1/(v_{hu}+\sigma_h)$, where v_{hm} is the hole volume where $g_n(1/v_h)$ has its maximum. We found that $(\gamma V^*/N'_h)\delta(1/v_h)$ decreases from 2.2 at 275 K to 1.5 at 320 K. This value can be compared with $\delta\ln\omega=2.0$, a value determined from the frequency distribution at 278 K. The observed correlation between $\varepsilon''(\ln\omega)$ and the hole size dispersion may show that the Cohen-Turnbull free volume theory of mobility also has some relevance when applied in a local approximation.

CONCLUSIONS

(i) We have found for a low molecular pure DGEBA resin that the hole free volume $V_f=V-V_{\rm occ}$ calculated from PVT experiments employing the Simha-Somcynsky lattice-hole theory is not the same for the same total volume $V(P,T)$ but differs for different P,T pairs. This behavior is caused by the occupied volume $V_{\rm occ}$, which shows almost no thermal expansion but is compressible. The variation of the specific hole free volume V_f can be described in a good approximation as a linear expansion with temperature, $V_f=E_f(T-T'_0)$, where the specific expansivity E_f decreases with the pressure P like $1/(1+aP)$. The fractional hole free volume, $h=V_f/V$, can be described by an Arrhenius equation with an enthalpy for the formation of vacancies (empty cells of the S-S lattice) of approximately half of the cohesive energy of the S-S lattice. These results correspond to previous findings for polymers.

(ii) The analysis of the positron lifetime spectra employing the new routine LT9.0 allowed us to separate three annihilation channels and to analyze successfully the distribution in the *o*-Ps lifetimes. The distribution is attributed to the static or dynamic free-volume hole size distribution of the DGEBA resin and used to calculate the mean, $\langle v_h\rangle$, and the mean dispersion, σ_h, of this distribution. From a comparison of $V_f=hV$ with $\langle v_h\rangle$ the mean hole density N'_h was estimated to be independent of the temperature [$N_h(300\text{ K})=N'_h/V=0.65$ nm^{-3}].

(iii) With decreasing temperature, the primary dielectric (a',a) relaxation and the viscosity in the temperature range above 285 K slow down faster than the shrinkage of the hole free volume V_f (or $\langle v_h\rangle$) would predict this on the basis of the classical free volume theory of Cohen and Turnbull. V_f becomes zero at approximately 23 K below the Vogel temperature T_0 of primary (a',a) relaxation, $T'_0\approx T_0-23$ K. Plots of the frequency $\log\omega$ versus $1/V_f$ can be linearized when taking into account this discrepancy by substituting $1/V_f$ by $1/(V_f-\Delta V)$ with $\Delta V=E_f(T_0-T'_0)$. This shows that not the entire specific hole free volume V_f is related to the primary relaxation process via the free volume theory, but a smaller portion, $V_f-\Delta V$. To explain this behavior, we have assumed that monovacancies in the S-S lattice may present too small a local free volume to show a liquidlike behavior and an activation energy is required for the cooperative rearranging of mers. Multivacancies may, however, show this behavior. The minimum size of these multivacancies for allowing the primary (a',a) relaxation was estimated to be in average ~1.5 of the volume of the S-S lattice cell. The analysis of the pressure dependency of the structural dynamics of DGEBA confirms this conclusion. Long chain molecules such as polymers seem to need larger vacancy agglomerates for showing a liquidlike behavior.

(iv) The spatial heterogeneity observed by PALS above T_g is caused by the volume fluctuations, which have a close

relation to the dynamic heterogeneity of the structural relaxation. From the dispersions in the *o*-Ps lifetimes, the mean fluctuation in the fractional free volume may be calculated. Using a fluctuation approach, the smallest representative freely fluctuating subsystem related to structural relaxation, $\langle V_{SV} \rangle$, is estimated from the hole size dispersion σ_h. This volume decreases with increasing temperature from ~ 7 nm^3 at T_g to 1.5 nm^3 at $T=1.2T_g$ in qualitative correspondence to estimates from heat capacity spectroscopy. Reasons for quantitative differences between the results of our method and the conclusion from dynamic heat capacity were discussed. A model was proposed that relates the spatial structure of the free volume as concluded from our PALS experiments to the known mobility pattern of the dynamic glass transition at low (cooperative α-relaxation) and high (a-relaxation) temperatures. Indications were found that the fluctuating free volume may be related to the dynamics of the liquid via the Cohen-Turnbull equation.

ACKNOWLEDGMENTS

We thank M. Beiner (Halle) and S. Corezzi (Perugia) for providing us with the sample and the dynamic data as well as for helpful comments. E. Donth (Halle, Dresden) is acknowledged for stimulating discussions on the general subject and his theory. We thank J. Kansy (Katowice) for delivering the new routine LT9.0 and D. Kilburn and S. Townrow (Bristol) for a critical reading the manuscript. One of us (E.M.H.) wishes to thank the Deutscher Akademischer Austauschdienst and the Martin-Luther-University Halle-Wittenberg for the support as a visiting scientist.

[1] E. Donth, *The Glass Transition: Relaxation Dynamics in Liquids and Disordered Materials* (Springer, Berlin, 2001).
[2] K. L. Ngai, J. Non-Cryst. Solids **275**, 7 (2000); in *Third International Symposium on Slow Dynamics in Complex Systems*, Sendai, Japan, 2003, AIP Conference Proceedings 708 edited by M. Tokuyana and I. Oppenheim (AIP, 2004), pp. 515; in *Nonlinear Dielectric Phenomena in Complex Liquids*, Proceedings of the NATO Advanced Research Workshop, Jaszowiec-Ustron, Poland, 2003, NATO Sciences Series II. Mathematics, Physics and Chemistry, Vol. 157, edited by S. J. Rzoska and V. P. Zhelezny (Kluwer, Dordrecht, The Netherlands, 2004), pp. 247–258.
[3] H. Sillescu, J. Non-Cryst. Solids **243**, 81 (1999).
[4] M. D. Edinger, C. A. Angell, and S. R. Nagel, J. Phys. Chem. **100**, 13200 (1996).
[5] W. Götze and L. Sjögren, Rep. Prog. Phys. **55**, 241 (1992).
[6] R. Zorn, J. Phys.: Condens. Matter **15**, R1025 (2003).
[7] J. T. Bendler, J. J. Fontanella, M. F. Shlesinger, J. Bartoš, O. Šauža, and J. Krištiak, Phys. Rev. E **71**, 031508 (2005).
[8] G. P. Johari and M. Goldstein, J. Chem. Phys. **74**, 2034 (1980).
[9] G. Adam and J. H. Gibbs, J. Chem. Phys. **43**, 139 (1965).
[10] T. G. Fox and P. J. Flory, J. Appl. Phys. **21**, 581 (1950); J. Polym. Sci. **14**, 315 (1954).
[11] A. K. Doolittle, J. Appl. Phys. **21**, 1471 (1951).
[12] F. Bueche, J. Chem. Phys. **21**, 1858 (1953); **24**, 418 (1956); **30**, 748 (1959).
[13] M. H. Cohen and D. Turnbull, J. Chem. Phys. **31**, 1164 (1959); D. Turnbull and M. H. Cohen, *ibid.* **52**, 3038 (1970).
[14] G. S. Grest and M. H. Cohen, Adv. Chem. Phys. **48**, 455 (1981).
[15] M. Paluch, J. Gapinski, A. Patkovski, and E. W. Fischer, J. Chem. Phys. **114**, 8048 (2001).
[16] M. Paluch, C. M. Roland, J. Gapinski, and A. Patkovski, J. Chem. Phys. **118**, 3177 (2003).
[17] C. M. Roland and R. Casalini, Macromolecules **36**, 1361 (2003).
[18] J. T. Bendler, J. J. Fontanella, M. F. Shlesinger, and M. C. Wintersgill, Electrochim. Acta **48**, 2267 (2003); **49**, 5249 (2004).
[19] G. Dlubek, D. Kilburn, and M. A. Alam, Electrochim. Acta **49**, 5241 (2004); **50**, 2351 (2005).
[20] G. Dlubek, D. Kilburn, and M. A. Alam, Macromol. Chem. Phys. **206**, 818 (2005).
[21] H. Vogel, Phys. Z. **22**, 645 (1921).
[22] G. S. Fulcher, J. Am. Ceram. Soc. **8**, 339 (1925).
[23] G. Tammann and W. Hesse, Z. Anorg. Allg. Chem. **156**, 245 (1926).
[24] M. L. Williams, R. F. Landel, and J. D. Ferry, J. Am. Chem. Soc. **77**, 3701 (1955).
[25] R. Simha and T. Somcynsky, Macromolecules **2**, 342 (1969).
[26] R. E. Robertson, in *Computational Modelling of Polymers*, edited by J. Bicerano (Marcel Dekker, Midland, MI, 1992), p. 297.
[27] L. A. Utracki and R. Simha, J. Polym. Sci., Part B: Polym. Phys. **39**, 342 (2001).
[28] L. A. Utracki and R. Simha, Macromol. Theory Simul. **10**, 17 (2001).
[29] L. A. Utracki and R. Simha, Polym. Int. **53**, 279 (2004).
[30] S. J. Tao, J. Chem. Phys. **56**, 5499 (1972).
[31] M. Eldrup, D. Lightbody, and J. N. Sherwood, Chem. Phys. **63**, 51 (1981).
[32] Y. C. Jean, Microchem. J. **42**, 72 (1990); in *Positron Annihilation*, Proceedings of the 10th International Conference, edited by Y.-J. He, B.-S. Cao, and Y. C. Jean [Mater. Sci. Forum 175–178, 59 (1995)].
[33] O. E. Mogensen, *Positron Annihilation in Chemistry* (Springer, Berlin, 1995).
[34] *Principles and Application of Positron and Positronium Chemistry*, edited by Y. C. Jean, P. E. Mallon, and D. M. Schrader (World Scientific, Singapore 2003).
[35] T. Goworek, K. Ciesielski, B. Jansińska, and J. Wawryszczuk, Chem. Phys. **230**, 305 (1998); B. Jasińska, A. E. Kozioł, and T. Goworek, *5th International Workshop on Positron and Positronium Chemistry (ppc 5)*, June 9–14, Lillafüred, Hungary, edited by Zs. Kajcsos, B. Lévay, and K. Süvegh [J. Radioanal. Nucl. Chem. 210, No. 2 (1996); 211, No. 1 (1996)].
[36] T. L. Dull, W. E. Frieze, D. W. Gidley, J. N. Sun, and A. F.

Yee, J. Phys. Chem. B **103**, 4657 (2001).
[37] R. B. Gregory, J. Appl. Phys. **70**, 4665 (1991).
[38] J. Liu, Q. Deng, and Y. C. Jean, Macromolecules **26**, 7149 (1993).
[39] G. Dlubek, V. Bondarenko, I. Y. Al-Qaradawi, D. Kilburn, and R. Krause-Rehberg, Macromol. Chem. Phys. **205**, 512 (2004).
[40] G. Dlubek, A. Sen Gupta, J. Pionteck, R. Krause-Rehberg, H. Kaspar, and K. H. Lochhaas, Macromolecules **37**, 6606 (2004).
[41] G. Dlubek, J. Wawryszczuk, J. Pionteck, T. Goworek, H. Kaspar, and K. H. Lochhaas, Macromolecules **38**, 429 (2005).
[42] R. Srithawatpong, Z. L. Peng, B. G. Olson, A. M. Jamieson, R. Simha, J. D. McGervey, T. R. Maier, A. F. Halasa, and H. Ishida, J. Polym. Sci., Part B: Polym. Phys. **37**, 2754 (1999).
[43] M. Schmidt and F. H. J. Maurer, Macromolecules **33**, 3879 (2000).
[44] G. Consolati, J. Phys. Chem. B **109**, 10096 (2005); G. Consolati, F. Quasso, R. Simha, and G. B. Olson, J. Polym. Sci., Part B: Polym. Phys. **43**, 2225 (2005).
[45] S. Corezzi, M. Beiner, H. Huth, K. Schröter, S. Capaccioli, R. Casalini, D. Fioretto, and E. Donth, J. Chem. Phys. **117**, 2435 (2002).
[46] M. Beiner and K. L. Ngai, Macromolecules **38**, 7033 (2005).
[47] S. Corezzi, P. A. Rolla, M. Paluch, J. Zioło, and D. Fioretto, Phys. Rev. E **60**, 4444 (1999); S. Corezzi, S. Capaccioli, R. Casalini, D. Fioretto, M. Paluch, and P. A. Rolla, Chem. Phys. Lett. **320**, 113 (2000).
[48] P. Zoller and C. J. Walsh, *Standard Pressure-Volume-Temperature Data for Polymers* (Technomic Publ Co, Inc., Lancaster, Basel 1995).
[49] J. Kansy, Nucl. Instrum. Methods Phys. Res. A **374**, 235 (1996).
[50] J. Kansy, LT for Windows, Version 9.0, Inst. of Phys. Chem. of Metals, Silesian University, Bankowa 12, PL-40–007 Katowice, Poland, March 2002 (private communication).
[51] R. K. Jain and R. Simha, J. Polym. Sci., Polym. Phys. Ed. **17**, 1929 (1979).
[52] R. K. Jain and R. Simha, J. Polym. Sci., Part B: Polym. Phys. **24**, 1247 (1986).
[53] Y. C. Jean, T. C. Sandreczki, and D. P. Ames, J. Polym. Sci. [A1] **24**, 1247 (1986).
[54] Q. Deng, F. Zandiehnadem, and Y. C. Jean, Macromolecules **25**, 1090 (1992).
[55] R. A. Venditti, J. K. Gillham, Y. C. Jean, and Y. Lou, J. Appl. Polym. Sci. **56**, 1207 (1995).
[56] F. Faupel, J. Kanzow, K. Günther-Schade, C. Nagel, P. Sperr, and G. Kögel, in *Positron Annihilation*, Proceedings of the 13th International Conference (ICPA-13), edited by T. Hyodo, Y. Kobayashi, Y. Nagashima, and H. Saito [Mater. Sci. Forum **445–446**, 219 (2004)].
[57] T. Kanaya, T. Tsukushi, K. Kaji, J. Bartoš, and J. Krištiak, Phys. Rev. E **60**, 1906 (1999).
[58] J. Bartoš, O. Šauša, P. Bandžuch, J. Zrubová, and J. Krištiak, J. Non-Cryst. Solids **307–310**, 417 (2002).
[59] K. L. Ngai, L.-R. Bao, A. F. Yee, and C. L. Sole, Phys. Rev. Lett. **87**, 215901 (2001).
[60] G. Dlubek, J. Stejny, and M. A. Alam, Macromolecules **31**, 4574 (1998).
[61] L. A. Utracki, Polym. Eng. Sci. **25**, 655 (1985).
[62] F. Stickel, E. W. Fischer, and R. Richert, J. Chem. Phys. **102**, 1 (1995); **104**, 2043 (1996).
[63] S. Vleeshouwers, J.-E. Kluin, J. D. McGervey, A. M. Jamieson, and R. Simha, J. Polym. Sci., Part B: Polym. Phys. **30**, 1429 (1992).
[64] K. Q. Yu, Z. S. Li, and J. Sun, Macromol. Theory Simul. **10**, 624 (2001).
[65] J. Bartoš and J. Krištiak, J. Non-Cryst. Solids **235–237**, 293 (1998).
[66] L. D. Landau and E. M. Lifshitz, *Statistical Physics* (Addison-Wesley, Reading, MA, 1958), pp. 352–356.
[67] J. H. Wendorff and E. W. Fischer, Kolloid Z. Z. Polym. **251**, 876 (1973).
[68] G. Meier, F. Kremer, G. Fytas, and A. Rizos, J. Polym. Sci., Part B: Polym. Phys. **34**, 1391 (1996).
[69] E. Donth, Acta Polym. **50**, 240 (1999).
[70] E. Hempel, G. Hempel, A. Hensel, C. Schick, and E. Donth, J. Phys. Chem. B **104**, 2460 (2000).
[71] E. Donth, E. Hempel, and C. Schick, J. Phys.: Condens. Matter **12**, L281 (2000).
[72] E. Donth, H. Huth, and M. Beiner, J. Phys.: Condens. Matter **13**, L451 (2001).
[73] E. Donth, Eur. Phys. J. E **12**, 11 (2003).
[74] U. Tracht, M. Wilhelm, A. Heuer, H. Feng, K. Schmidt-Rohr, and H. W. Spiess, Phys. Rev. Lett. **81**, 272 (1998).
[75] S. H. Glarum, J. Chem. Phys. **33**, 639 (1960).
[76] M. von Laue, Phys. Z. **18**, 542 (1917).
[77] E. Donth, J. Phys. I **6**, 1189 (1996).